

Palladium(II) Pincer Complexes of a C,C,C-NHC, Diphosphonium Bis(Ylide) Ligand

Rachid Taakili, Christine Lepetit, Carine Duhayon, Dmitry A. Valyaev, Noël Lugan,
Yves Canac*

LCC–CNRS, Université de Toulouse, CNRS, Toulouse, France

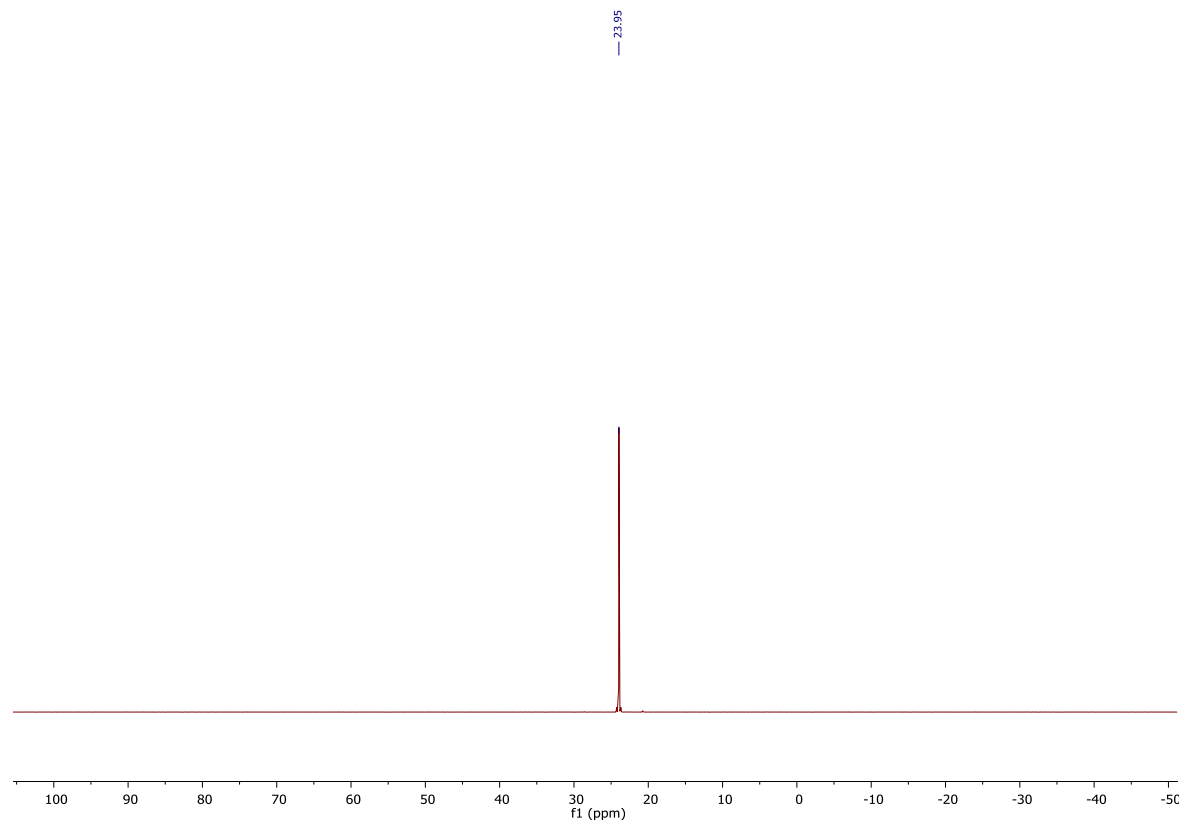
E-mail: yves.canac@lcc-toulouse.fr

Supporting Information

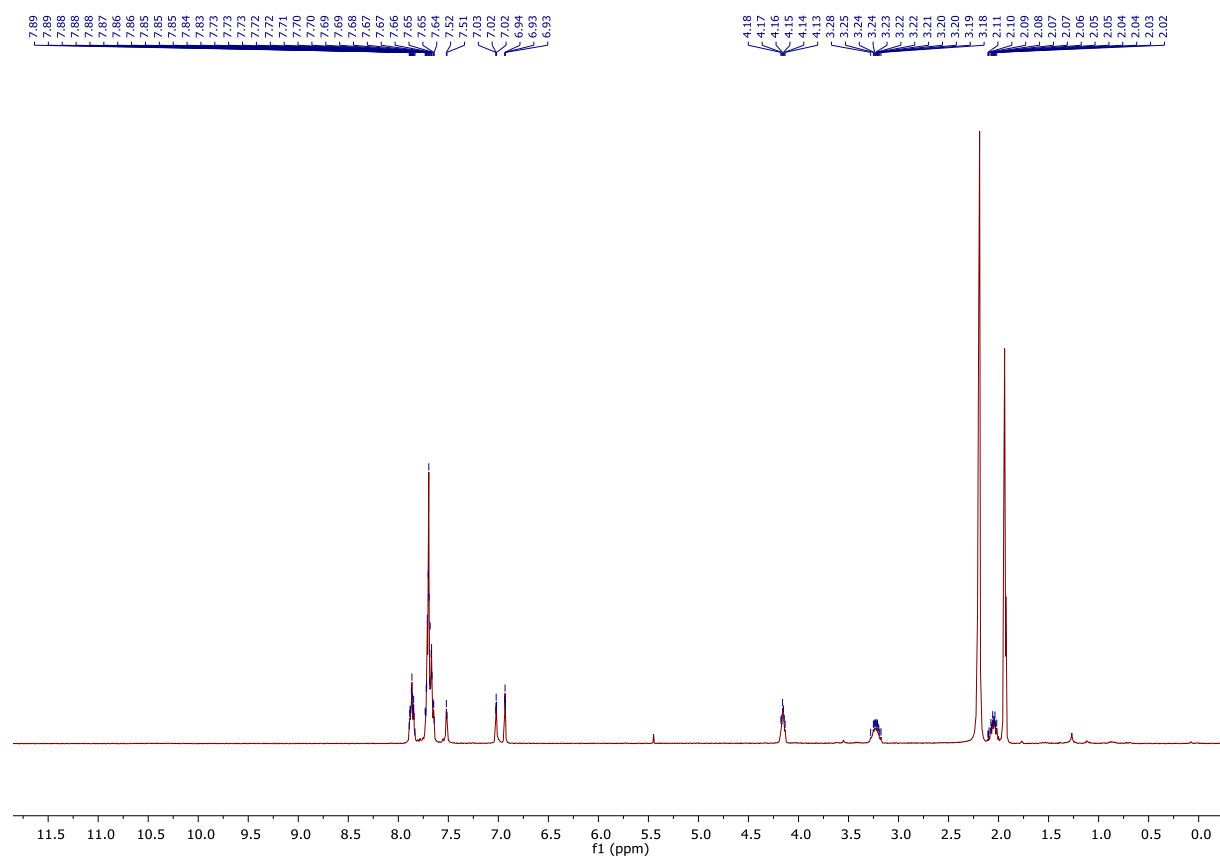
Table of contents

- NMR spectra of [2]Br	P-1
- NMR spectra of [3]Br ₃	P-3
- NMR spectra of [3](OTf) ₃	P-5
- NMR spectra of [4](OTf) ₂	P-6
- NMR spectra of [5](OTf) ₂	P-8
- NMR spectra of [6](OTf) ₂	P-9
- NMR spectra of [7](OTf)	P-11
- NMR spectra of [8](OTf) ₂	P-12
- NMR spectra of [9](OTf) ₂	P-14
- NMR spectra of [10](OTf) ₂	P-16
- Crystallographic table for [2](Br), [3](OTf) ₃ , [4](OTf) ₂ , [5](OTf) ₂ , <i>meso</i> -[9](OTf) ₂ , and <i>dl</i> -[9](OTf) ₂	P-17
- Computational details	P-18
- Optimized structure of complex 7 ⁺	P-18
- Optimized structure of complex 8 ²⁺	P-18
- Optimized structure of complex 8' ²⁺	P-19

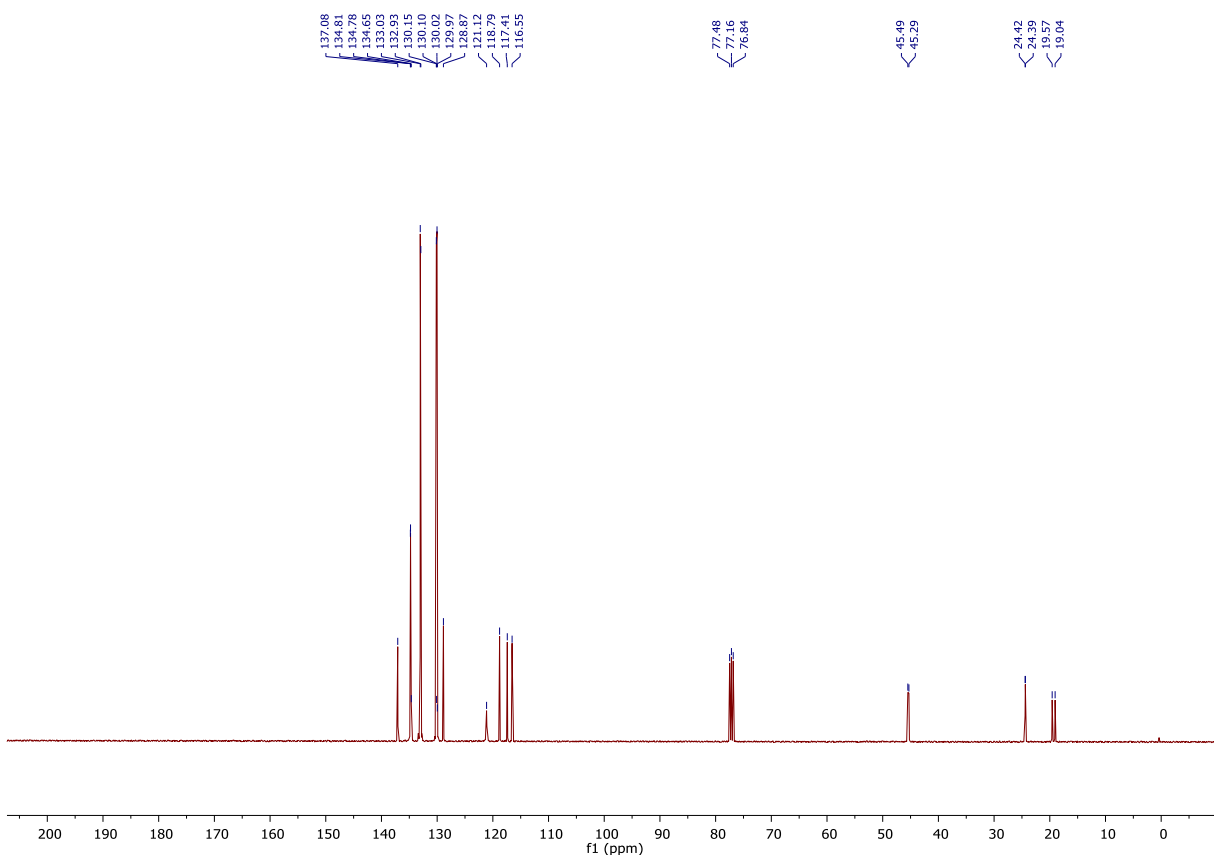
$^{31}\text{P}\{\text{H}\}$ NMR spectrum of [2]Br (in CDCl_3)



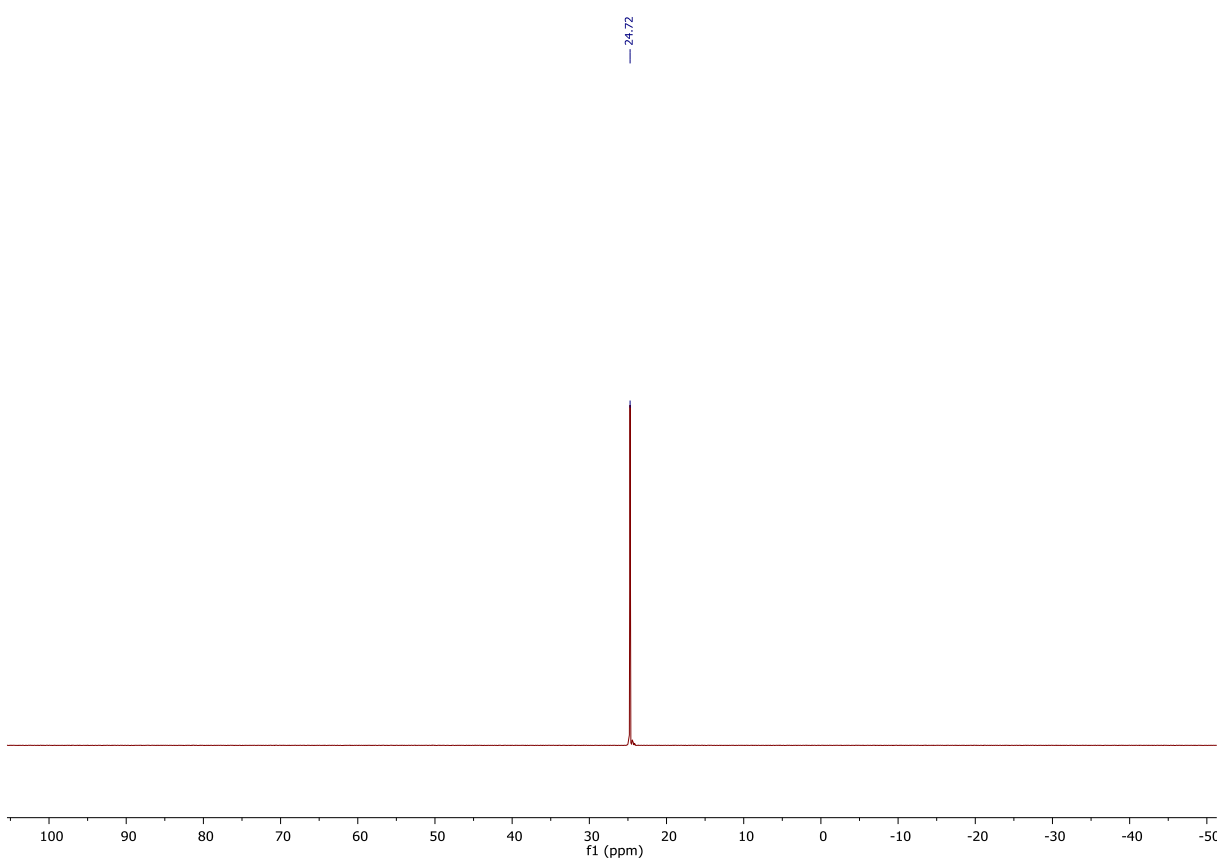
^1H NMR spectrum of [2]Br (in CDCl_3)



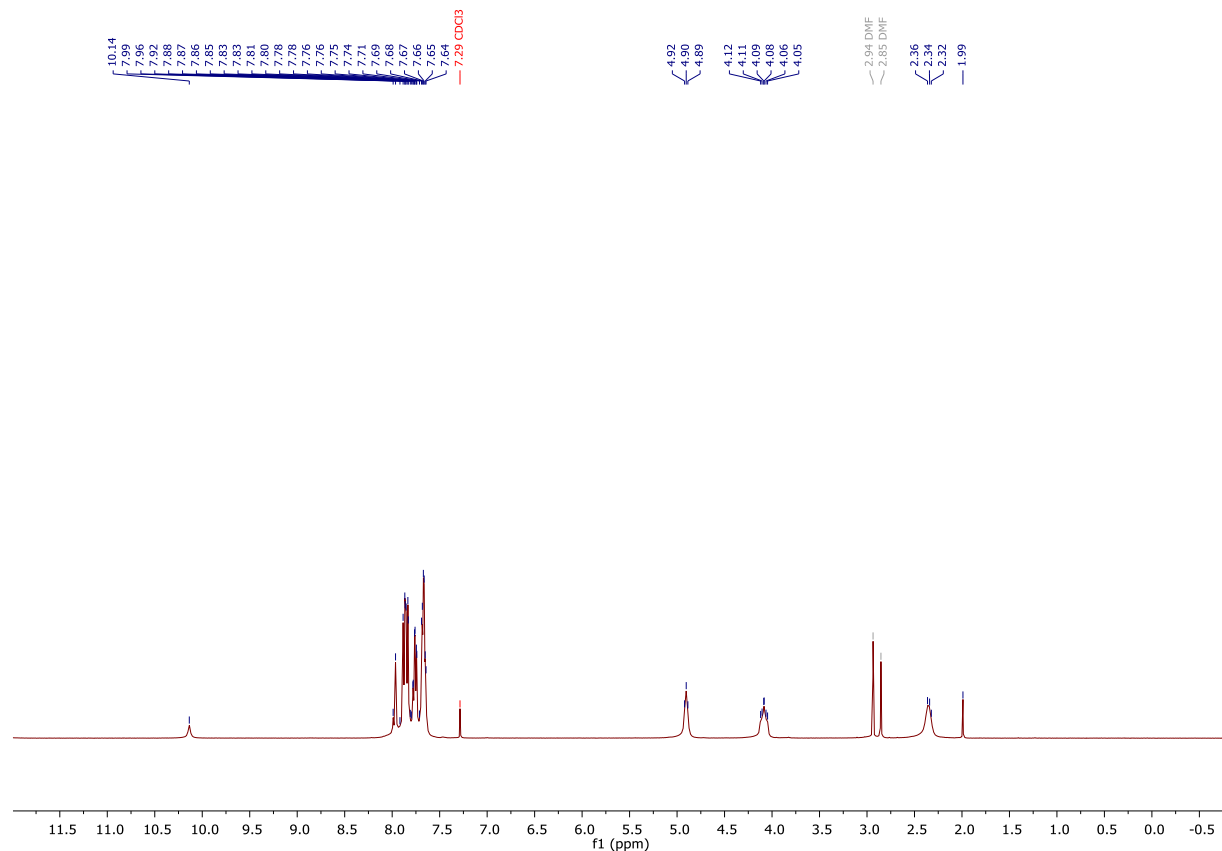
¹³C{¹H} NMR spectrum of [2]Br (in CDCl₃)



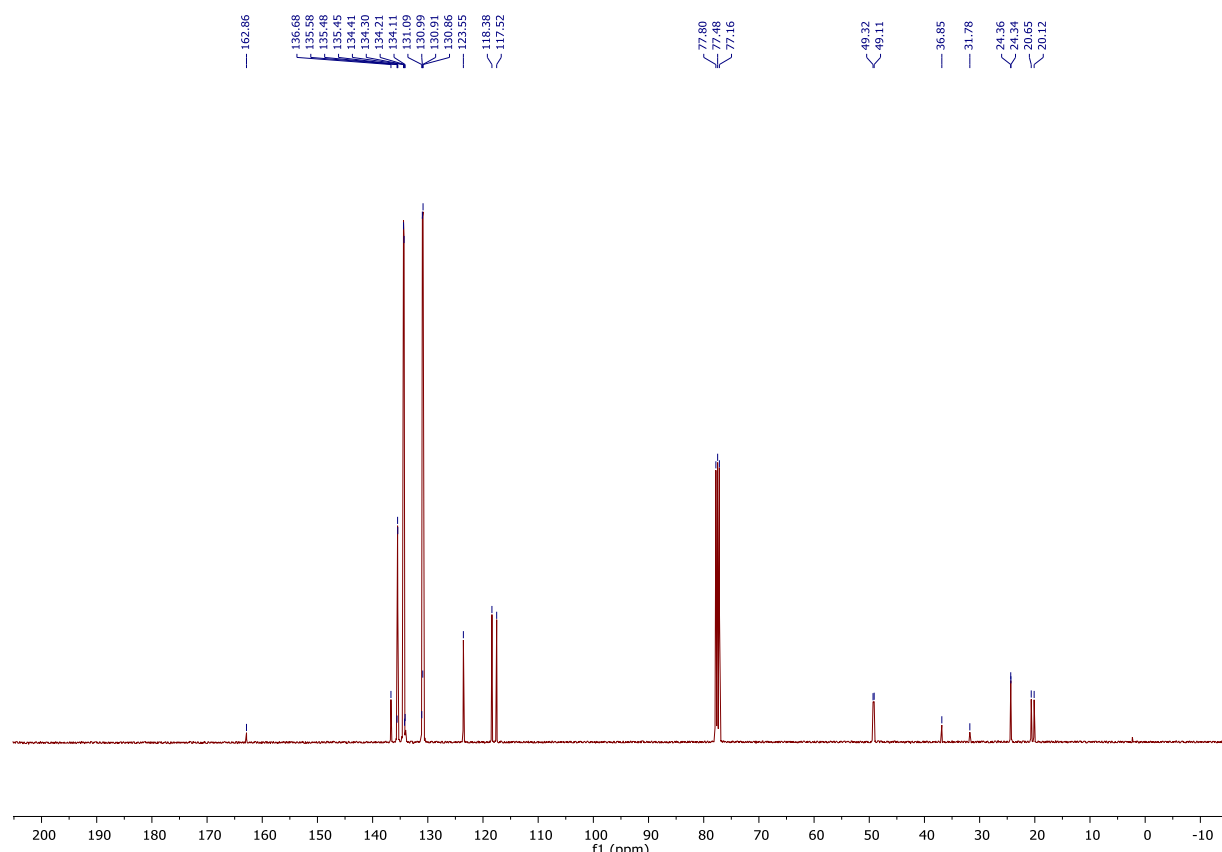
³¹P{¹H} NMR spectrum of [3]Br₃ (in CDCl₃)



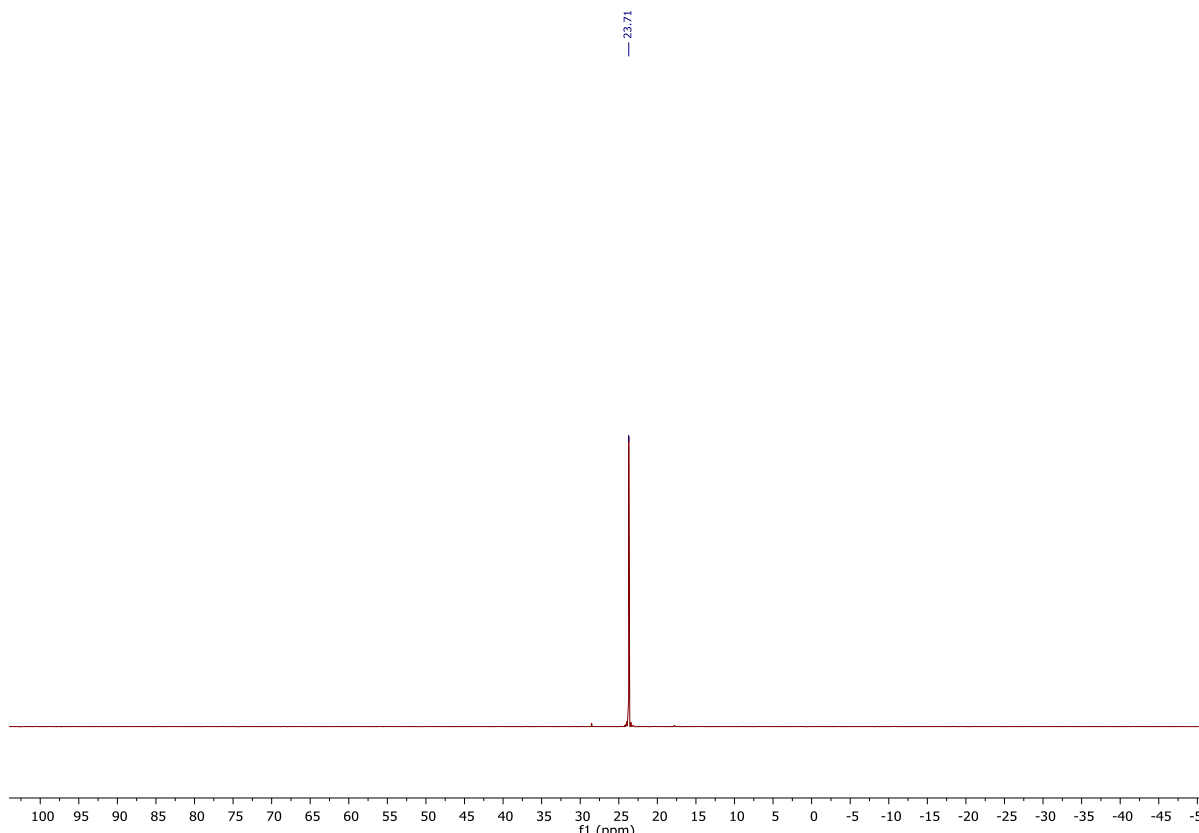
^1H NMR spectrum of [3]Br₃ (in CDCl₃)



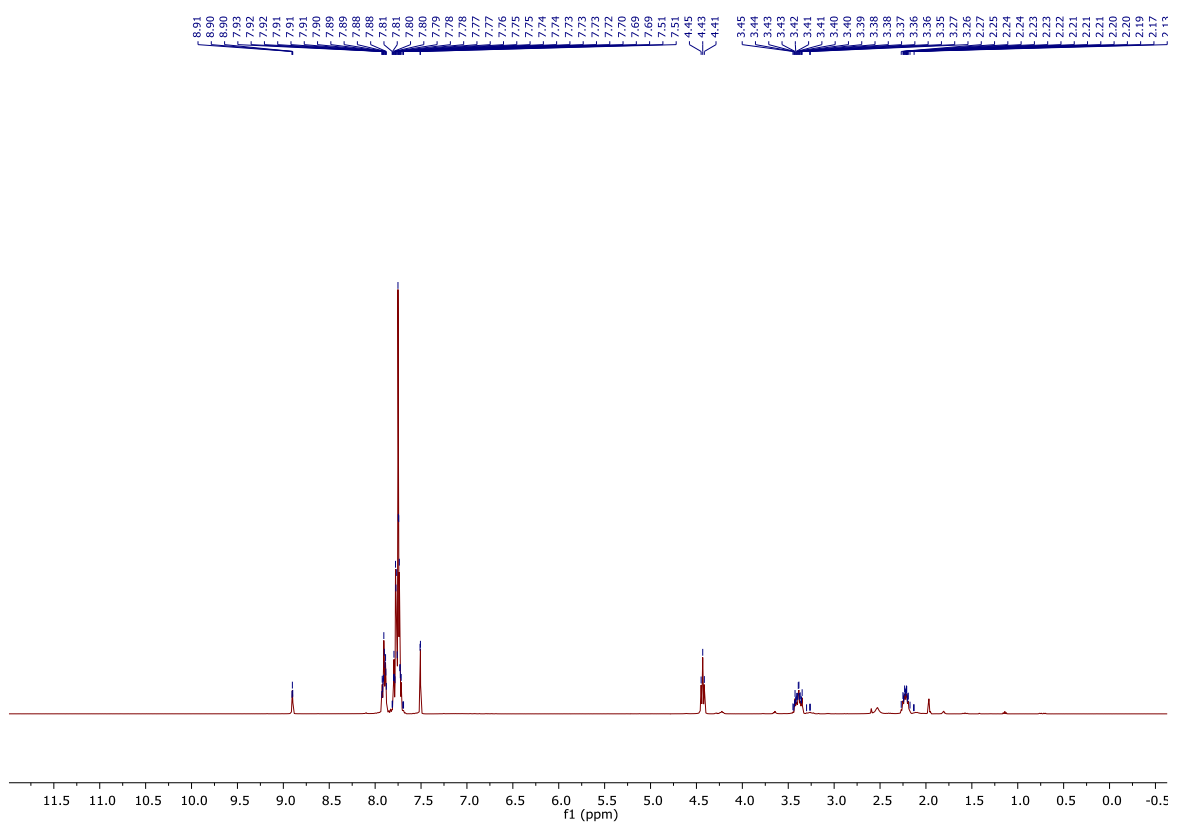
$^{13}\text{C}\{^1\text{H}\}$ NMR spectrum of [3]Br₃ (in CDCl₃)



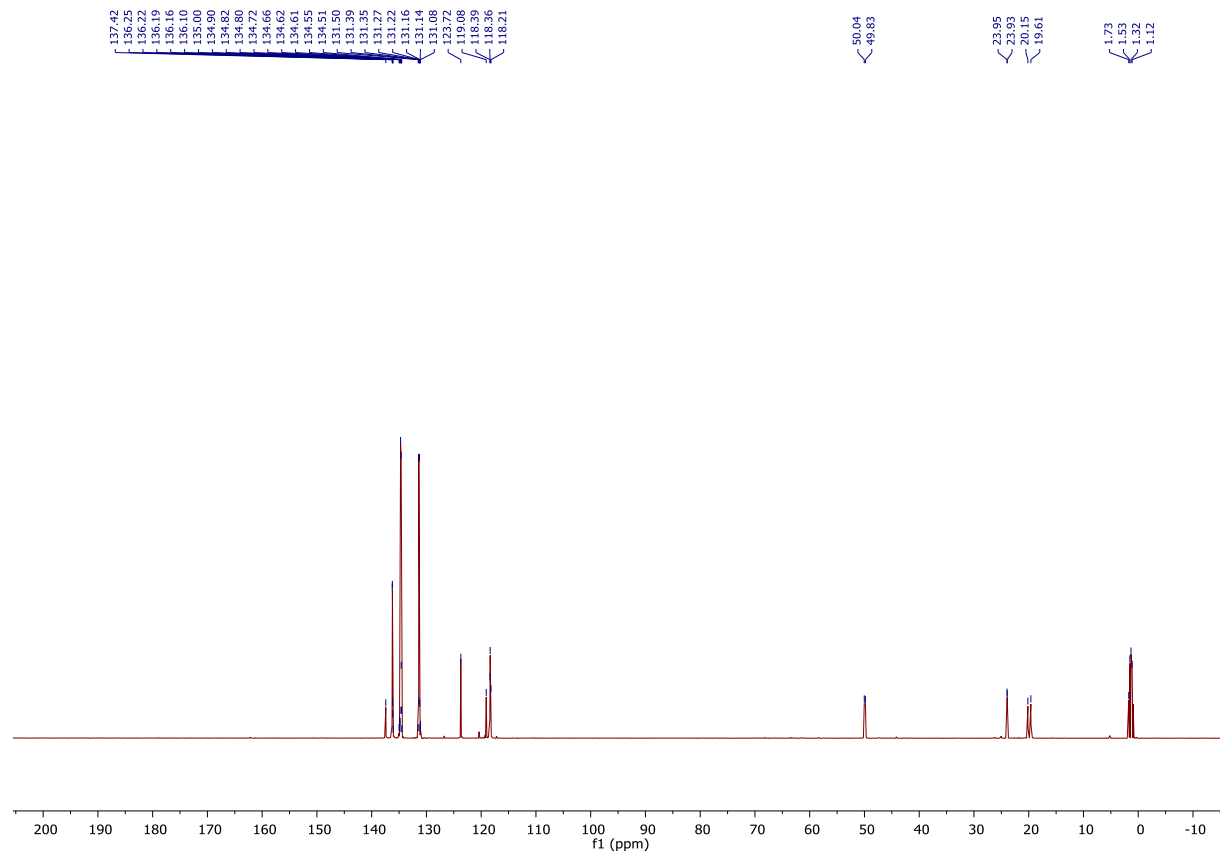
$^{31}\text{P}\{\text{H}\}$ NMR spectrum of [3](OTf)₃ (in CD₃CN)



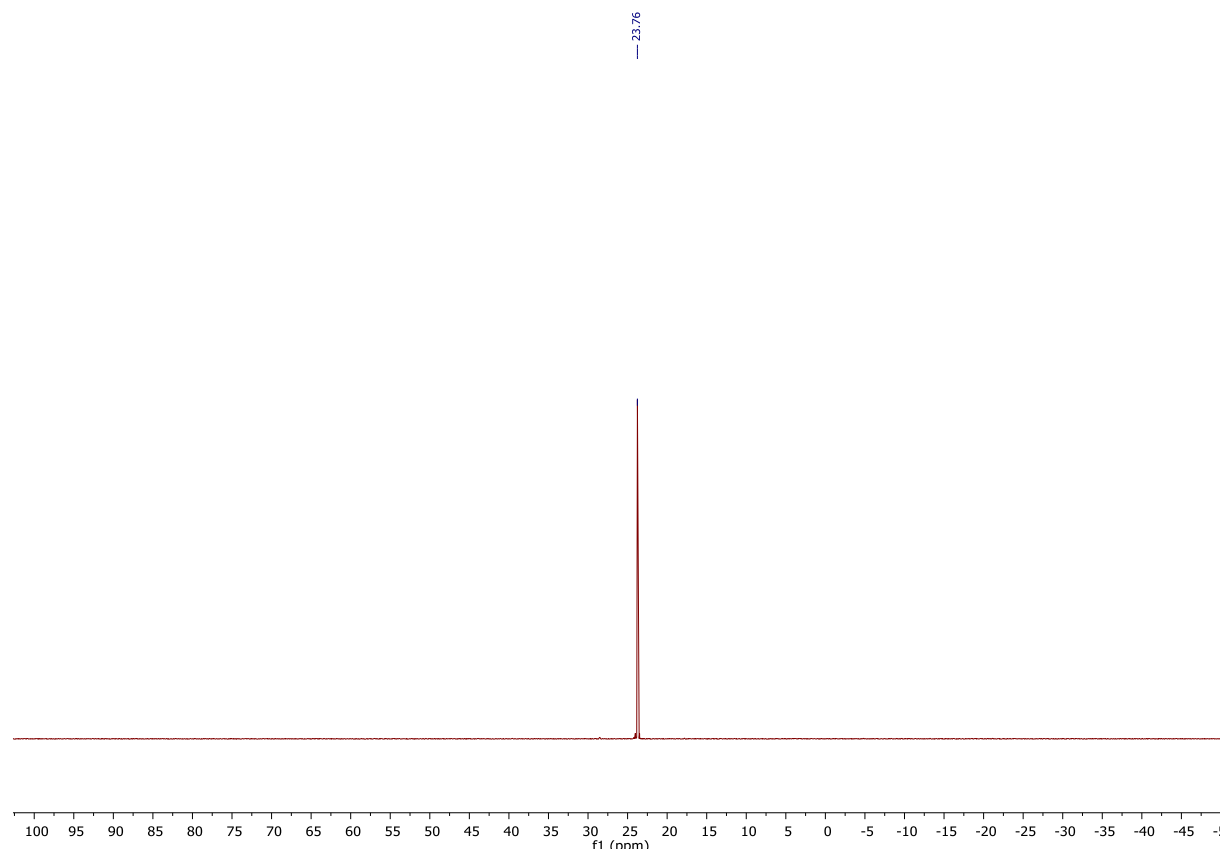
^1H NMR spectrum of [3](OTf)₃ (in CD₃CN)



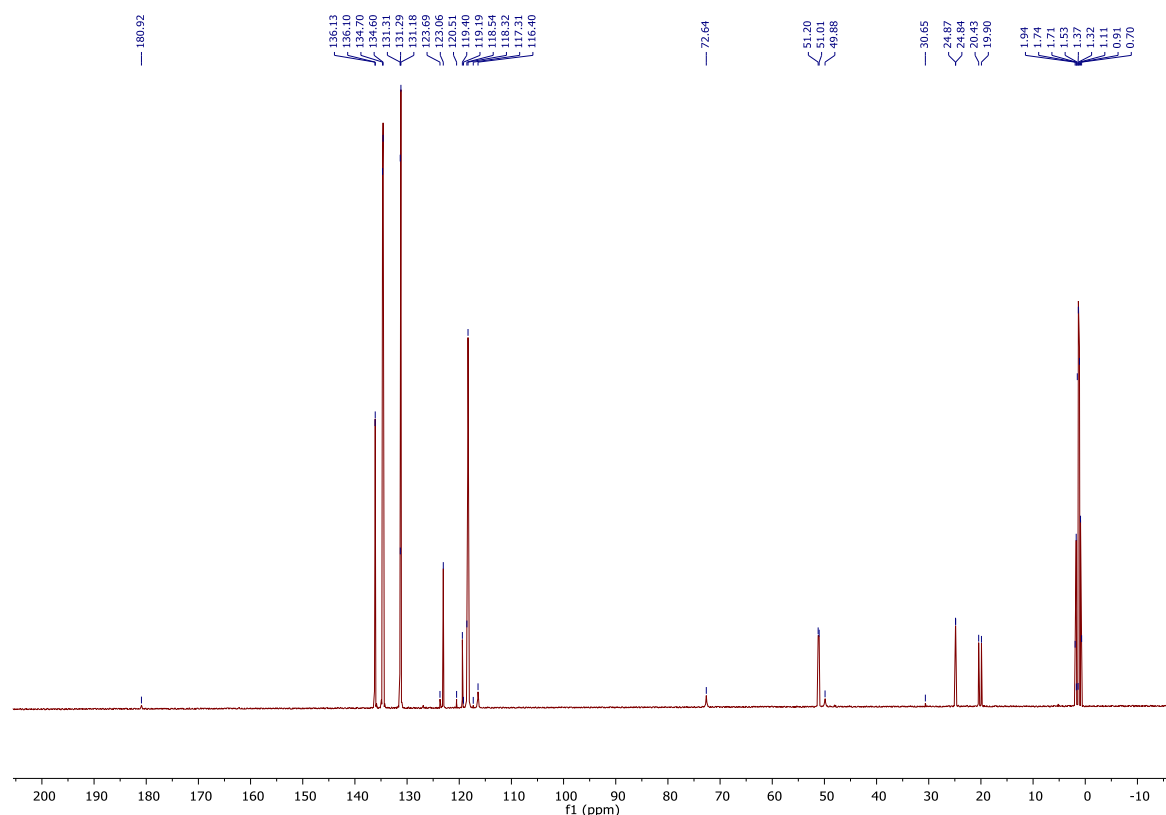
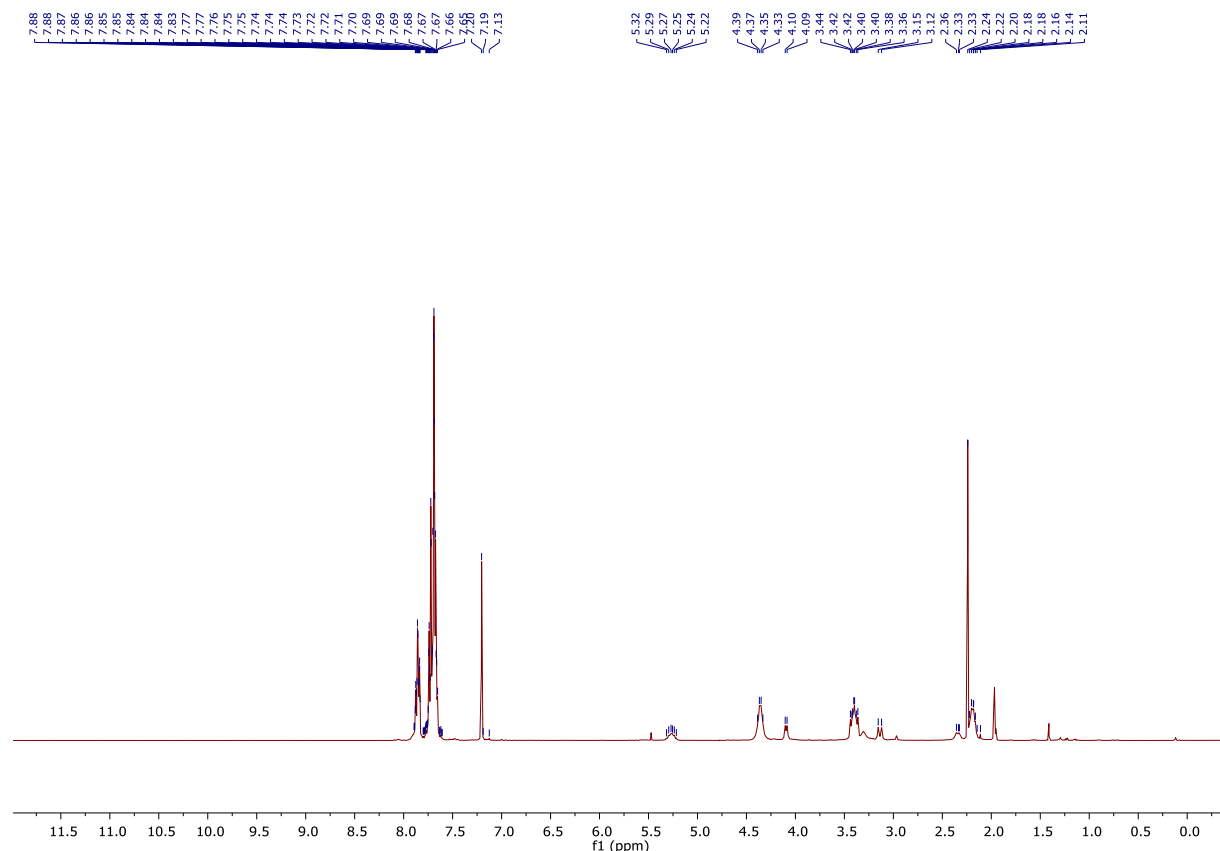
$^{13}\text{C}\{\text{H}\}$ NMR spectrum of [3](OTf)₃ (in CD₃CN)



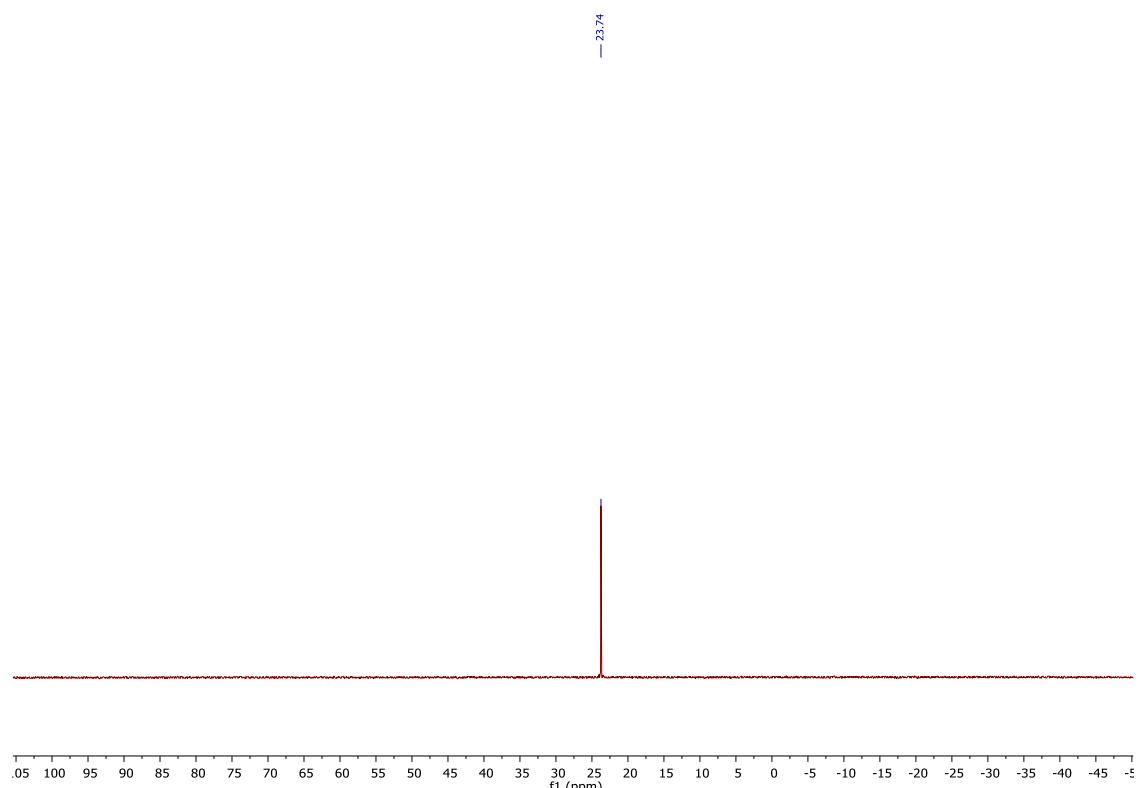
$^{31}\text{P}\{\text{H}\}$ NMR spectrum of [4](OTf)₂ (in CD₃CN)



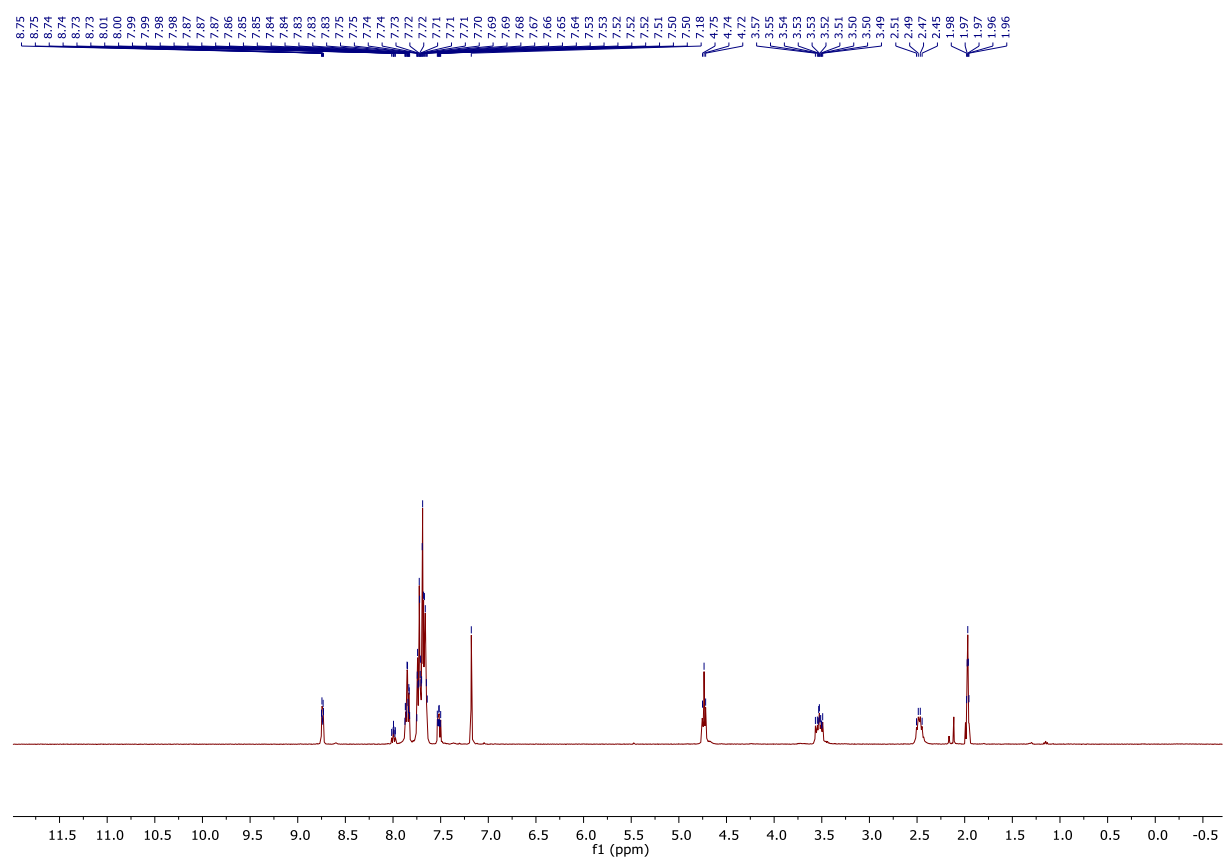
^1H NMR spectrum of [4](OTf)₂ (in CD₃CN)



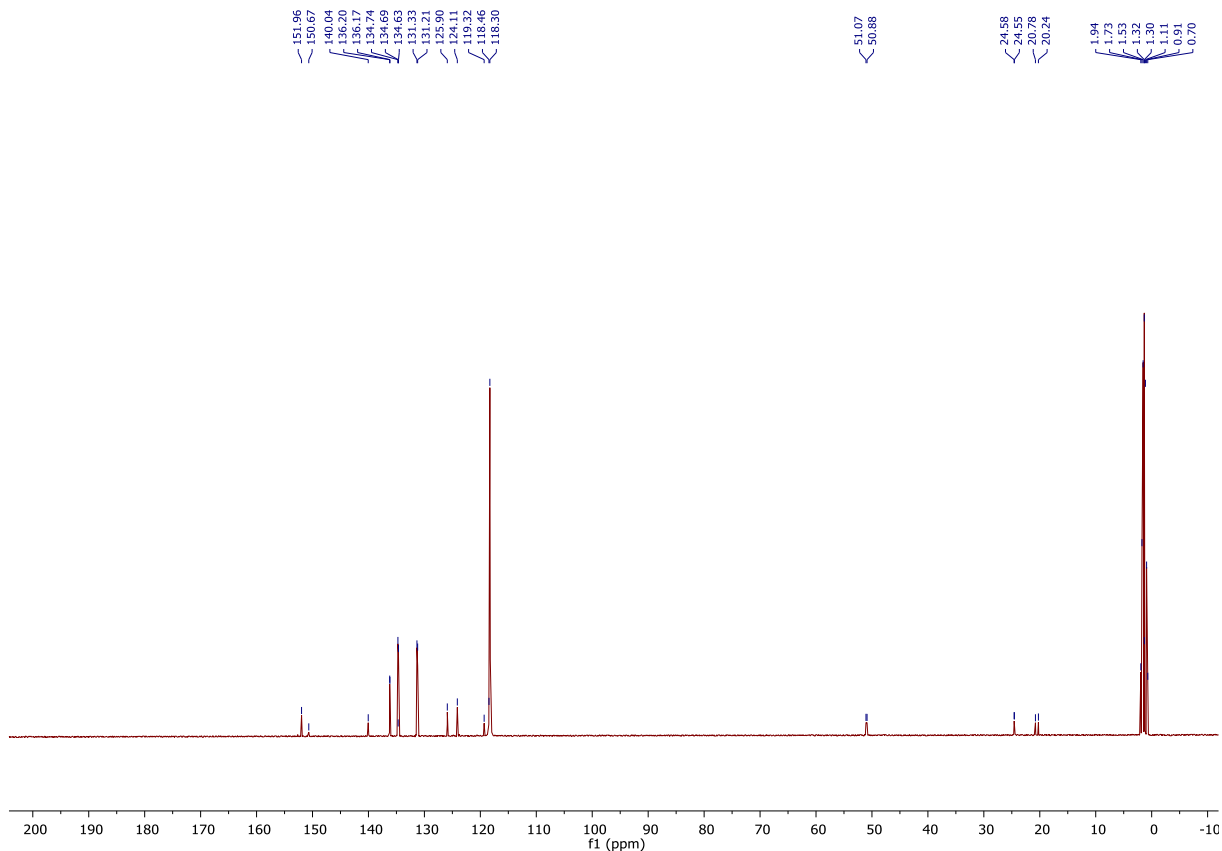
$^{31}\text{P}\{\text{H}\}$ NMR spectrum of [5](OTf)₂ (in CD₃CN)



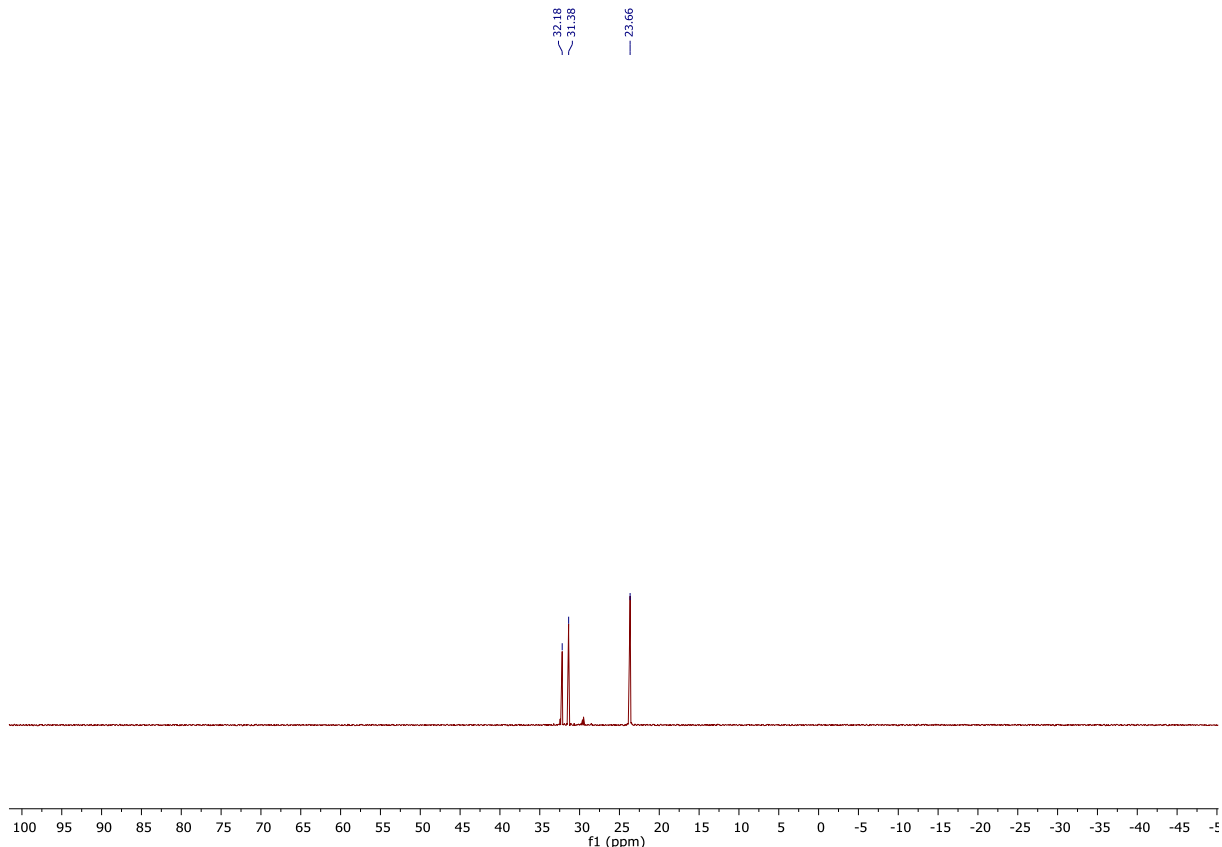
^1H NMR spectrum of [5](OTf)₂ (in CD₃CN)



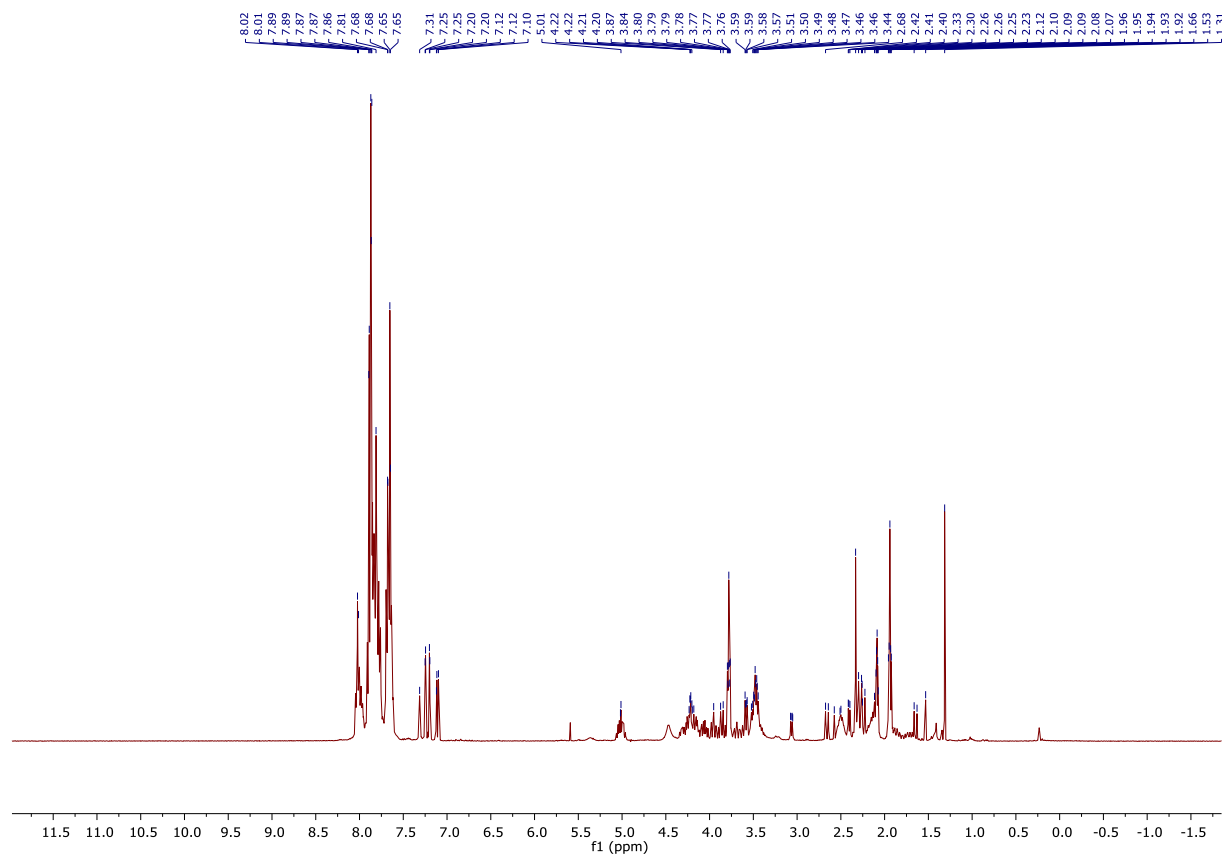
$^{13}\text{C}\{\text{H}\}$ NMR spectrum of [5](OTf)₂ (in CD₃CN)



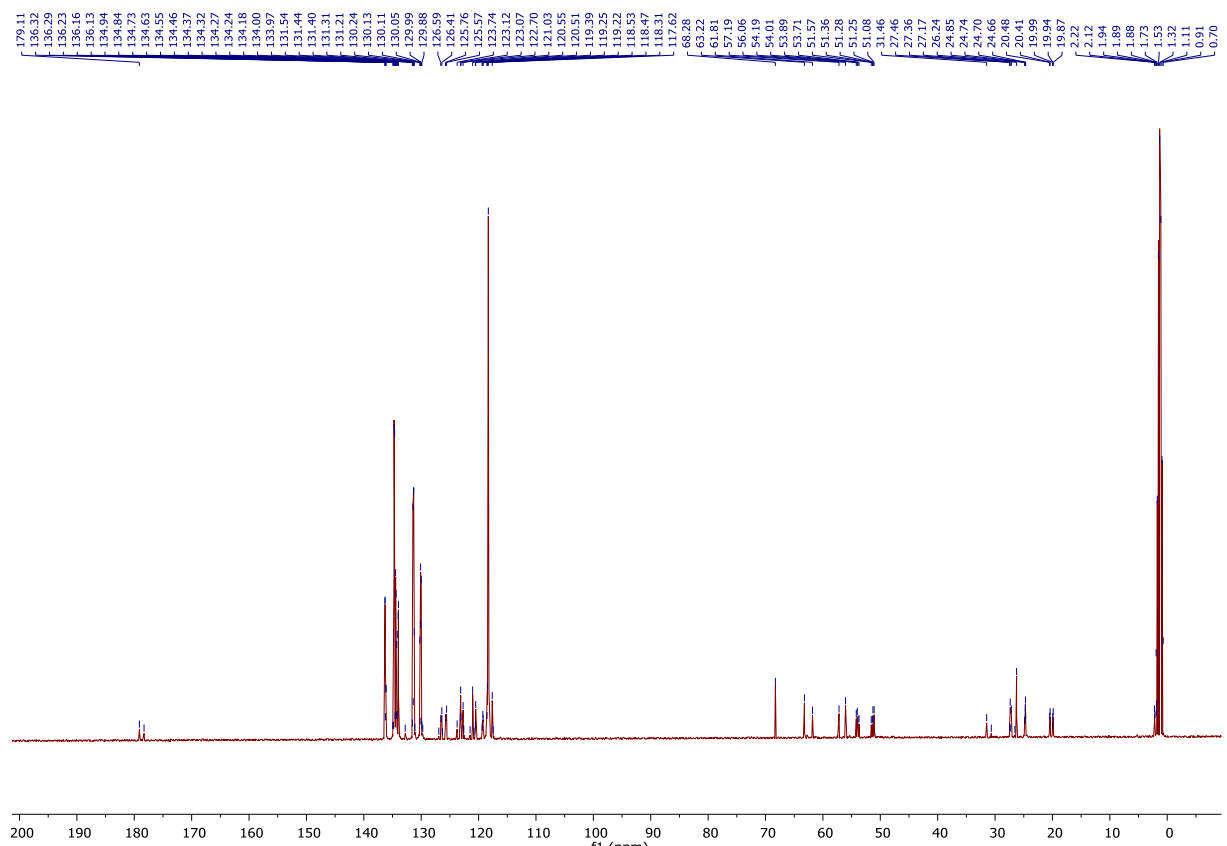
$^{31}\text{P}\{\text{H}\}$ NMR spectrum of [6](OTf)₂ (in CD₃CN)



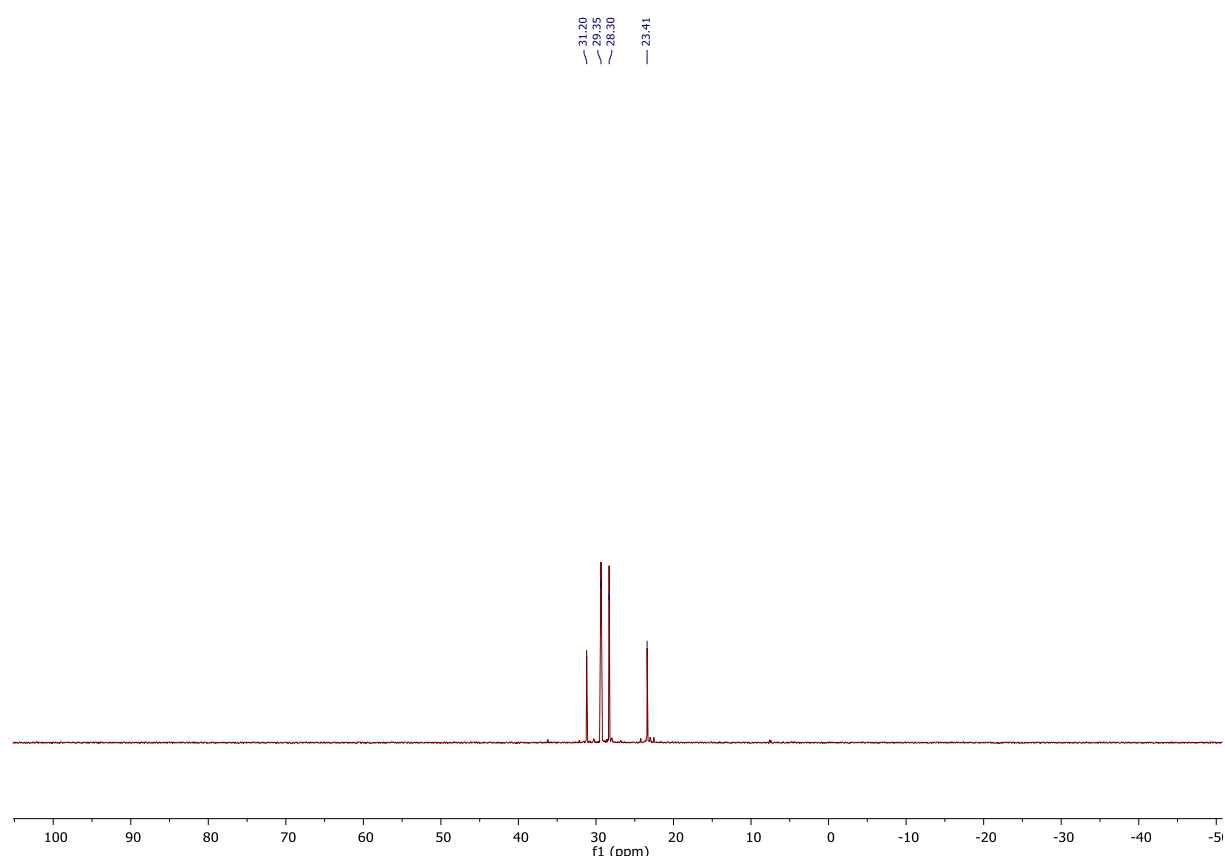
¹H NMR spectrum of [6](OTf)₂ (in CD₃CN)



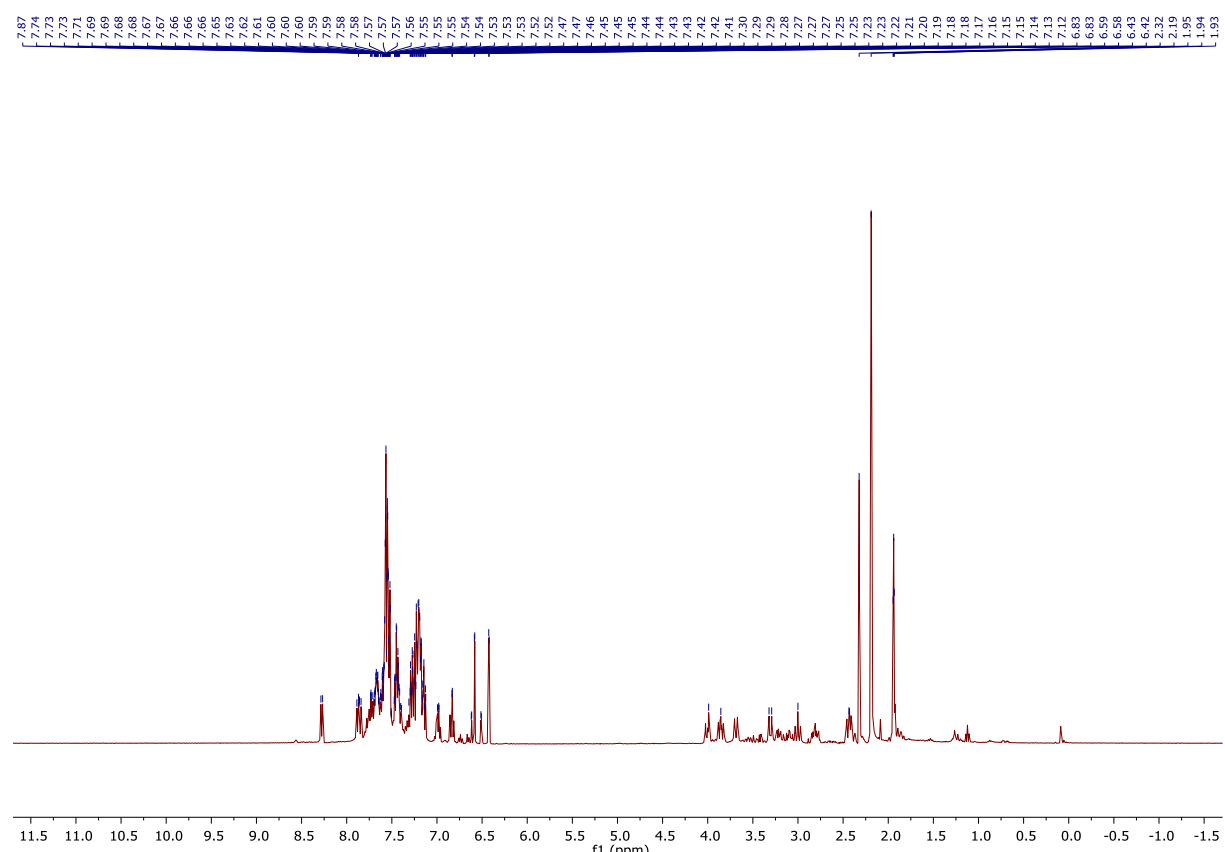
¹³C{¹H} NMR spectrum of [6](OTf)₂ (in CD₃CN)



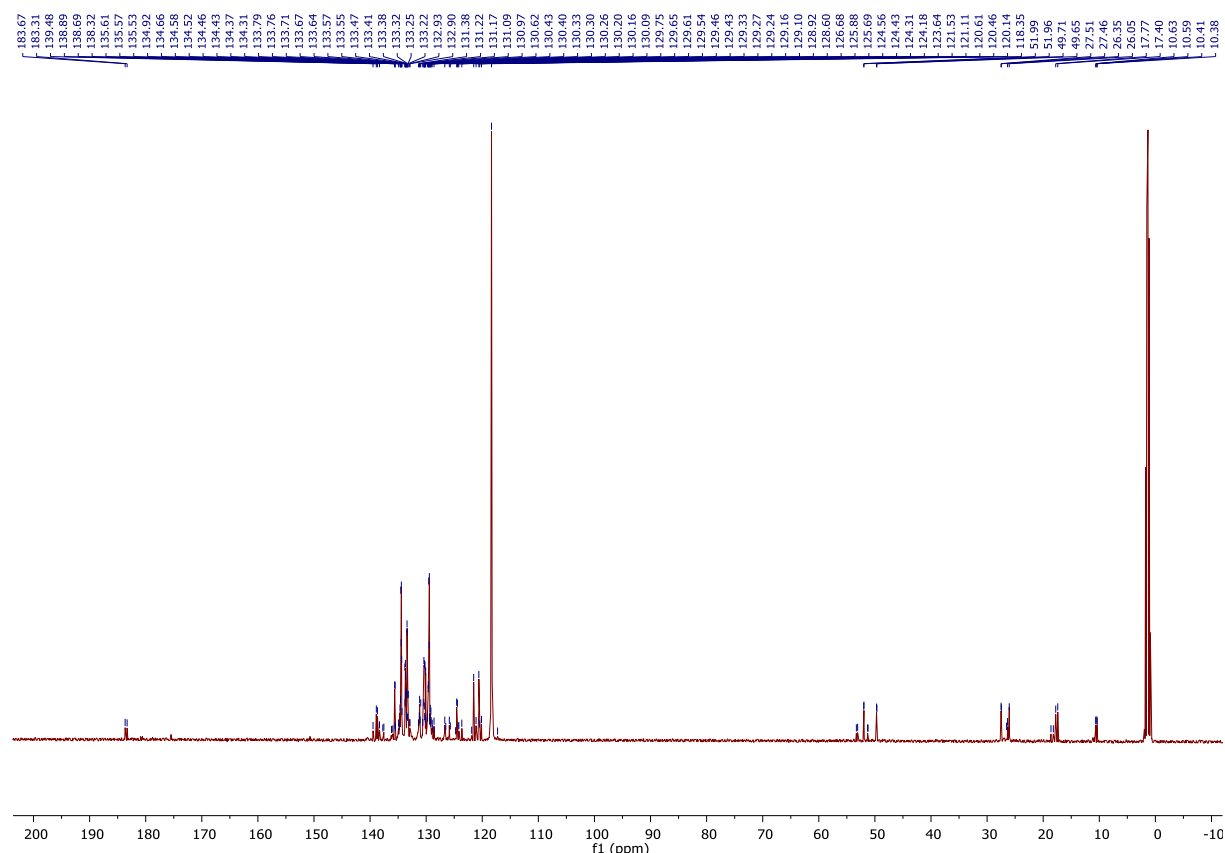
$^{31}\text{P}\{\text{H}\}$ NMR spectrum of [7](OTf) (in CD₃CN)



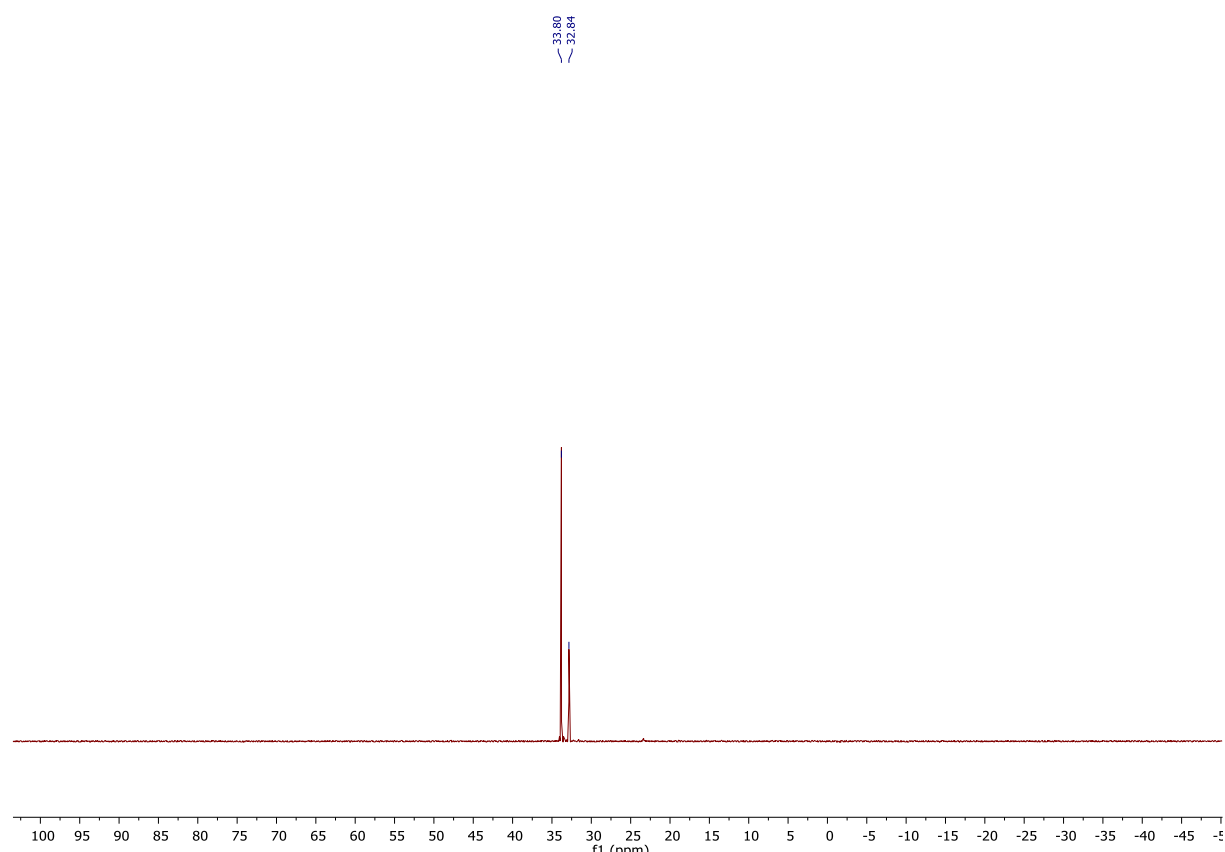
^1H NMR spectrum of [7](OTf) (in CD₃CN)



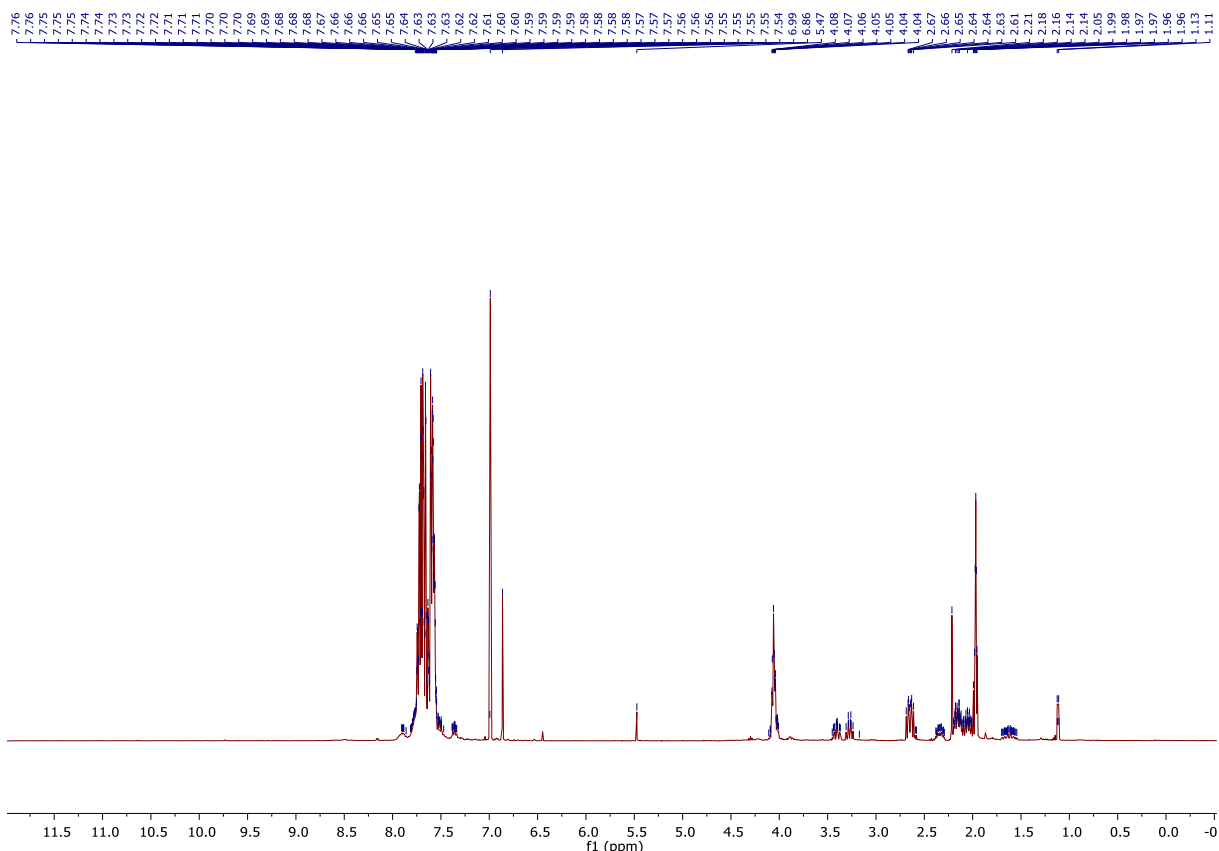
$^{13}\text{C}\{\text{H}\}$ NMR spectrum of [7](OTf) (in CD₃CN)



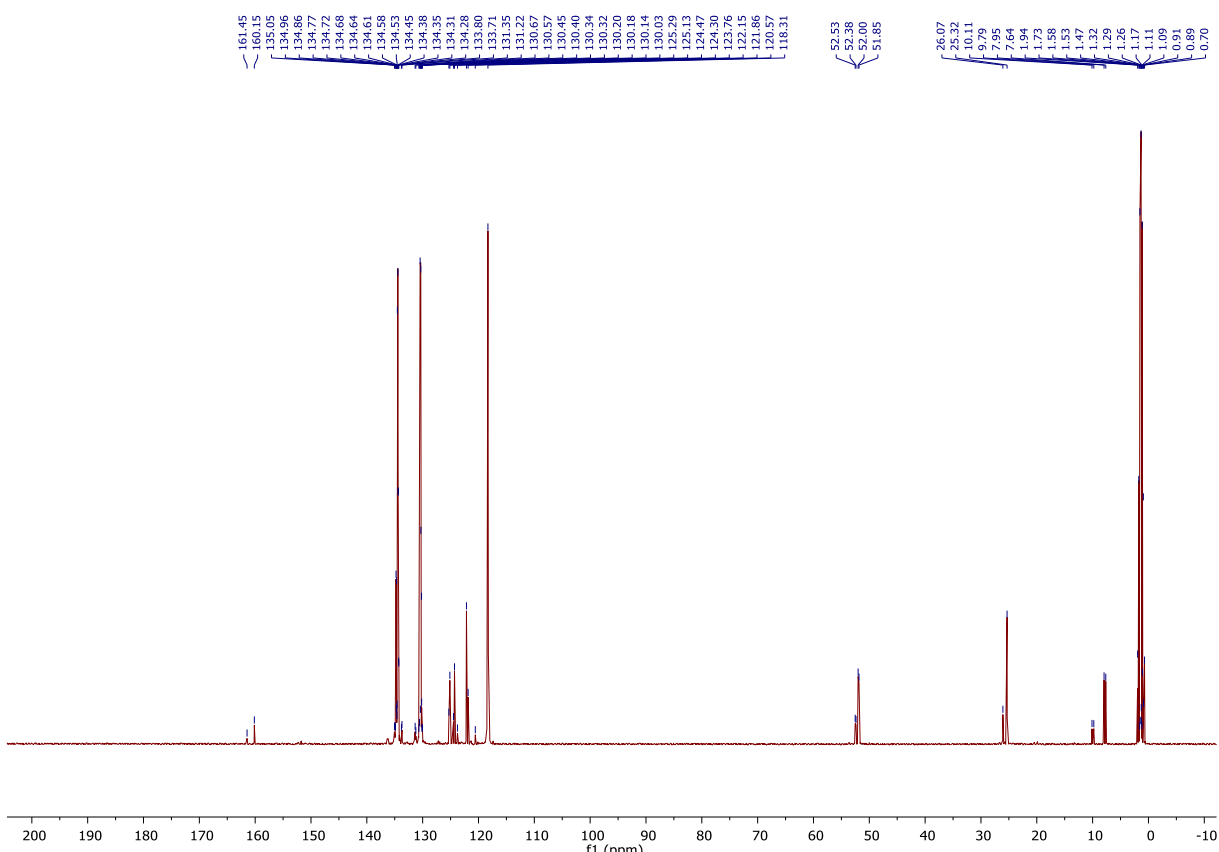
$^{31}\text{P}\{\text{H}\}$ NMR spectrum of [8](OTf)₂ (in CD₃CN)



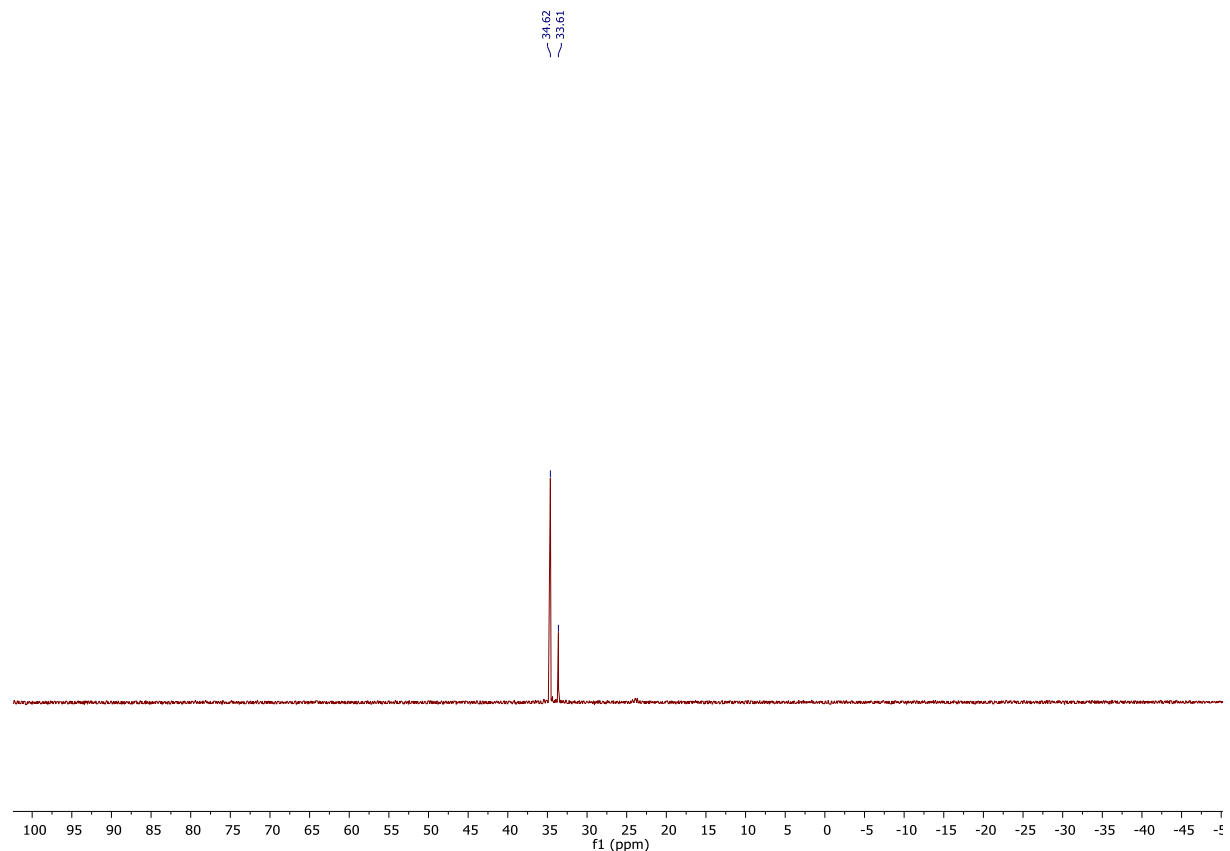
¹H NMR spectrum of [8](OTf)₂ (in CD₃CN)



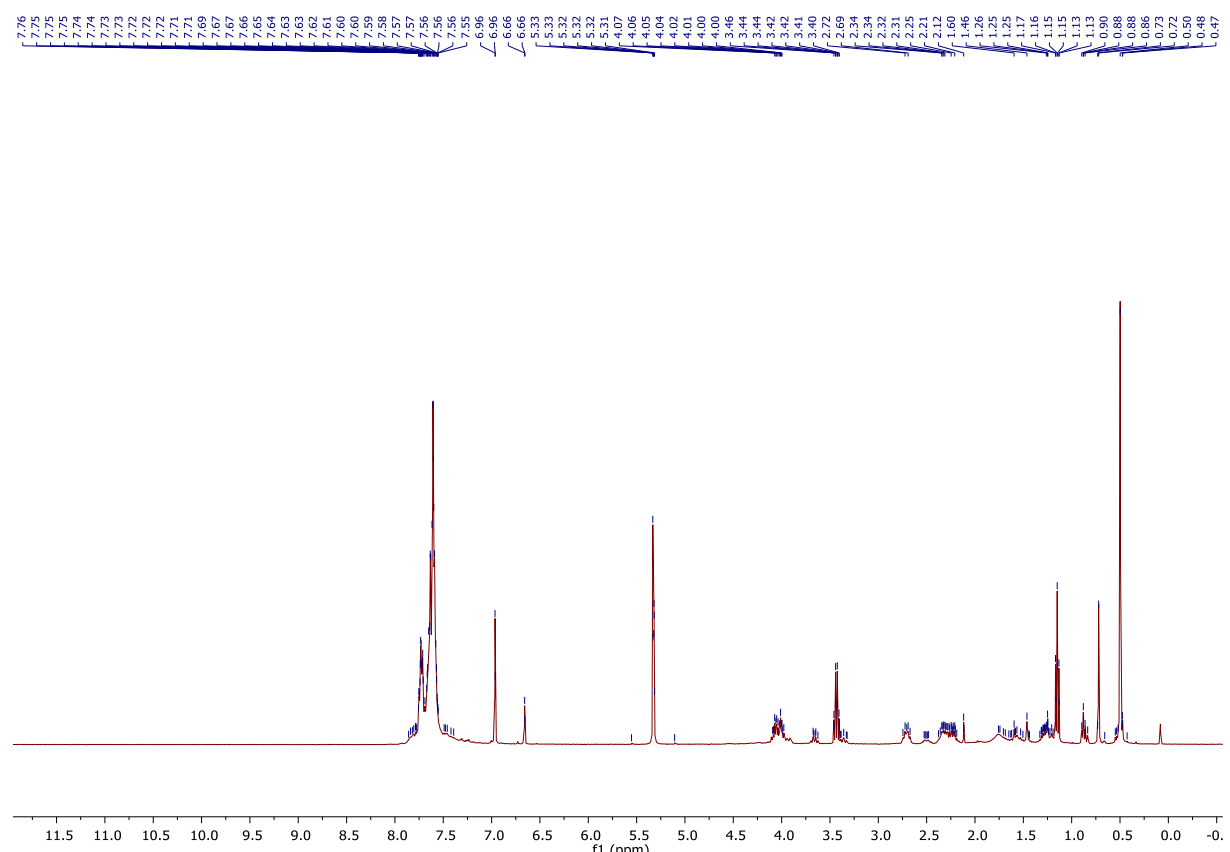
¹³C{¹H} NMR spectrum of [8](OTf)₂ (in CD₃CN)



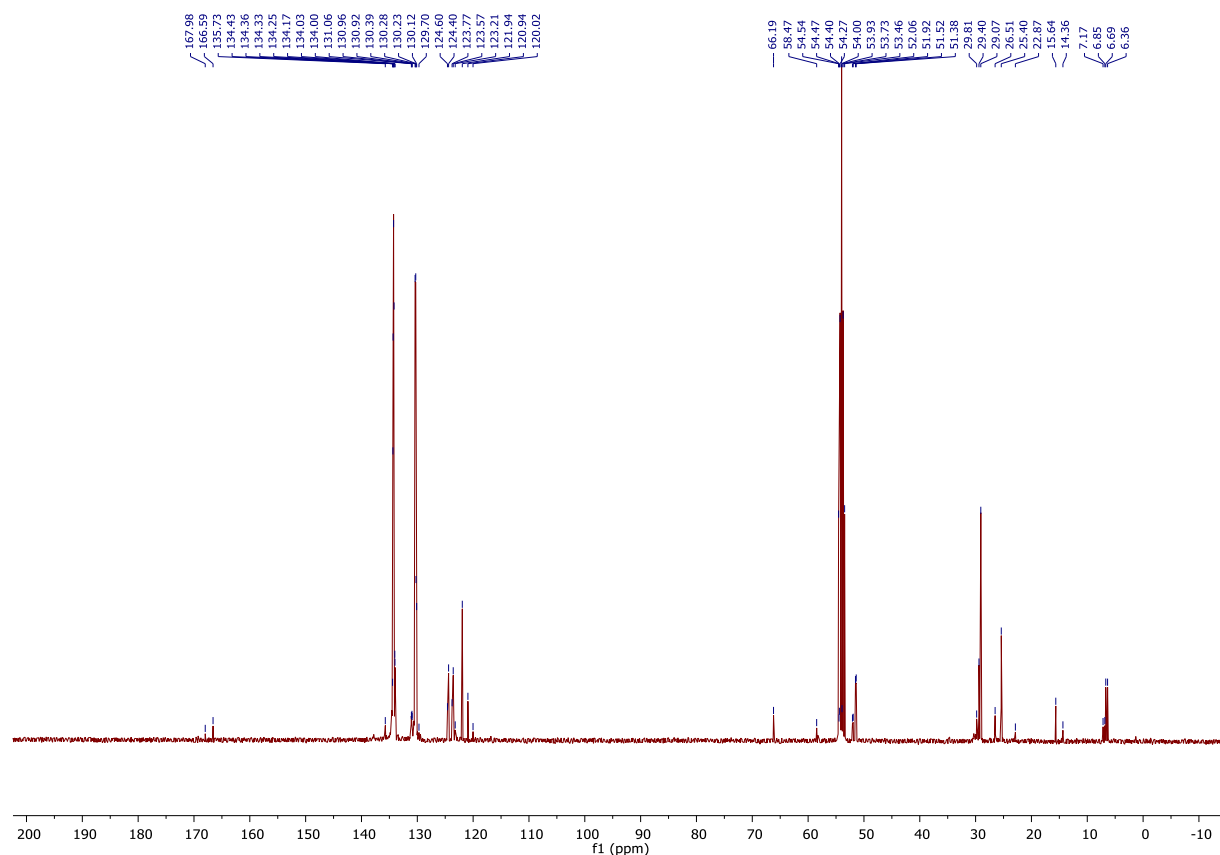
$^{31}\text{P}\{\text{H}\}$ NMR spectrum of [9](OTf)₂ (in CD₂Cl₂)



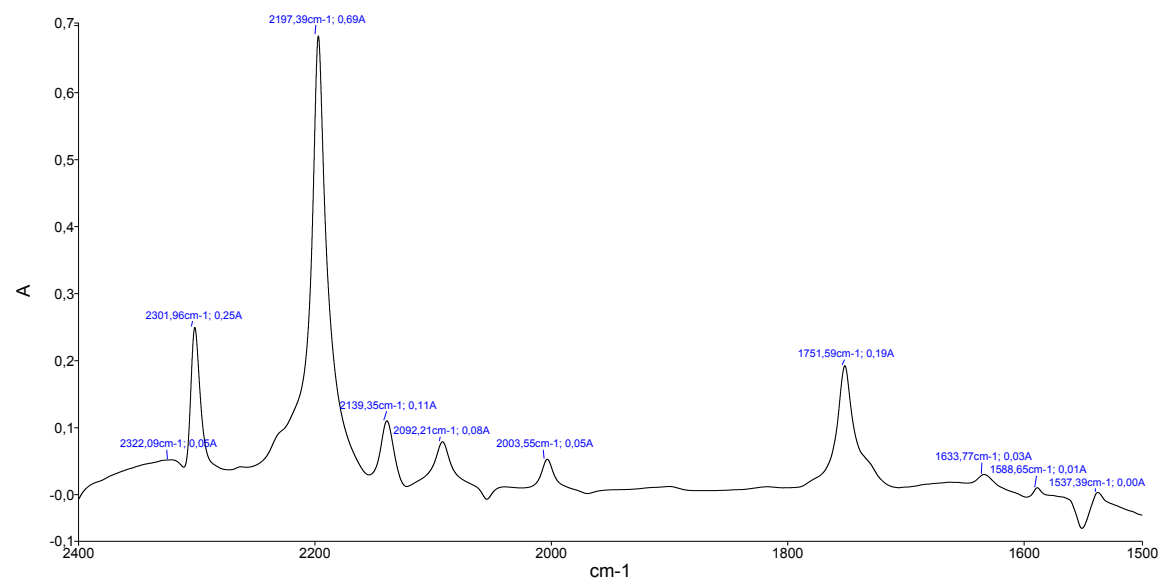
^1H NMR spectrum of [9](OTf)₂ (in CD₂Cl₂)



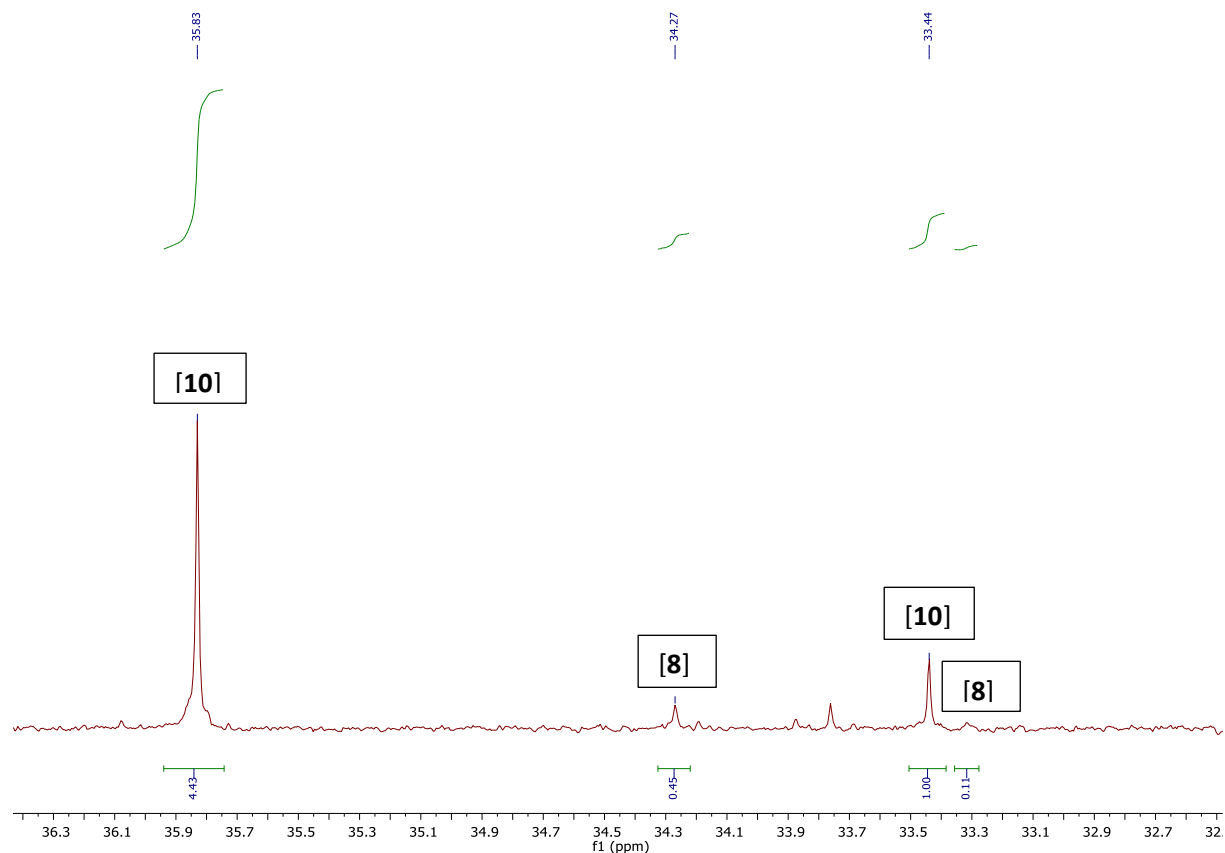
$^{13}\text{C}\{\text{H}\}$ NMR spectrum of [9](OTf)₂ (in CD₂Cl₂)



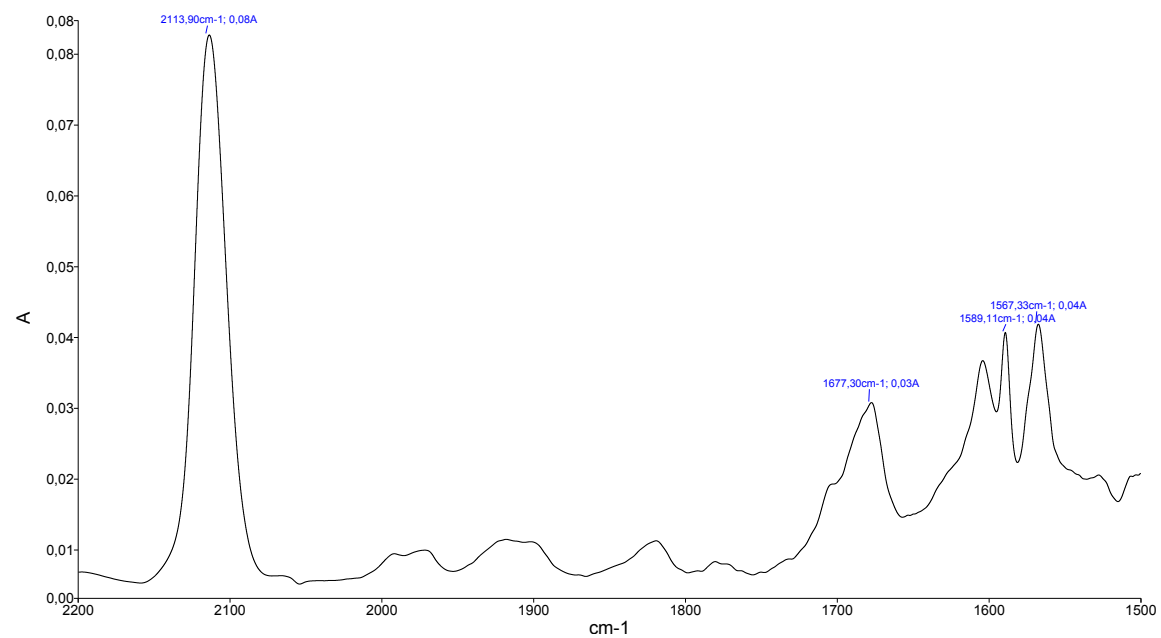
IR spectrum of [9](OTf)₂ (in CH₂Cl₂)



$^{31}\text{P}\{\text{H}\}$ NMR spectrum of [10](OTf)₂ (in CD₂Cl₂): 90% conversion.



IR spectrum of [10](OTf)₂ (in CH₂Cl₂)



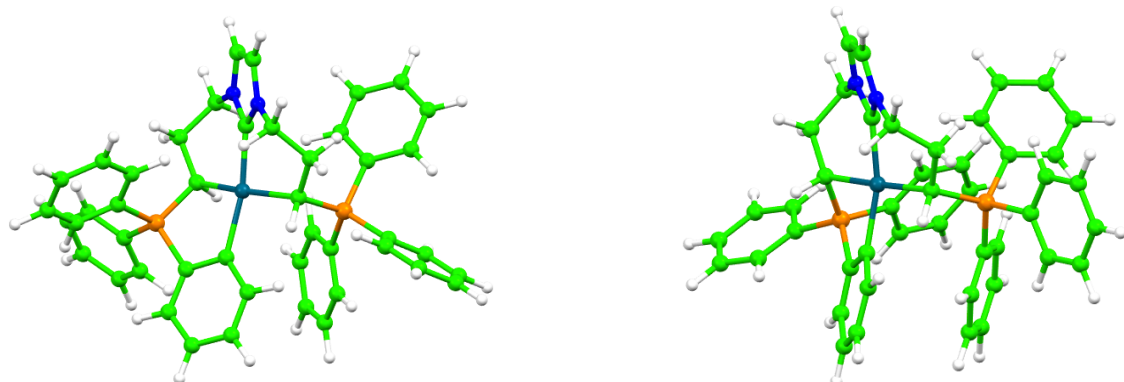
Crystallographic table for [2](Br), [3](OTf)₃, [4](OTf)₂, [5](OTf)₂, *meso*-[9](OTf)₂, and *dl*-[9](OTf)₂

	[2]Br	[3](OTf) ₃	[4](OTf) ₂	[5](OTf) ₂	<i>meso</i> -[9](OTf) ₂	<i>dl</i> -[9](OTf) ₂
Empirical formula	C ₂₄ H ₂₄ BrN ₂ P	C ₄₈ H ₄₅ F ₉ N ₂ O ₉ P ₂ S ₃	C ₅₄ H ₅₄ ClF ₆ N ₄ O ₆ P ₂ PdS ₂	C ₅₂ H ₄₇ Cl ₂ F ₆ N ₃ O ₆ P ₂ PdS ₂	C ₅₂ H ₅₁ F ₆ N ₃ O ₆ P ₂ PdS ₂	C ₅₂ H _{52.2} F ₆ N ₃ O _{6.60} P ₂ PdS ₂
Formula moiety	C ₂₄ H ₂₄ N ₂ P, Br	C ₄₅ H ₄₅ N ₂ P ₂ , 3(CF ₃ O ₃ S)	C ₄₈ H _{48.45} ClN ₂ P ₂ Pd, 2(CF ₃ O ₃ S), 2(C ₂ H ₃ N)	C ₅₀ H ₄₇ Cl ₂ N ₃ P ₂ Pd, 2(CF ₃ O ₃ S)	C ₅₀ H ₅₁ N ₃ P ₂ Pd, 2(CF ₃ O ₃ S), 0.6(H ₂ O)	C ₅₀ H ₅₁ N ₃ P ₂ Pd, 2(CF ₃ O ₃ S), 0.6(H ₂ O)
Formula mass	451.35	1122.98	1237.42	1227.29	1160.46	1171.27
Crystal system	orthorhombic	triclinic	triclinic	monoclinic	triclinic	monoclinic
Space group	P b c a	P -1	P -1	C 2/c	P -1	P 2 ₁ /n
T [K]	100	100	100	173	100	100
a [Å]	15.3294(6)	10.000(7)	12.9726(6)	25.8085(10)	12.7979(6)	13.6658(9)
b [Å]	15.1363(6)	13.831(10)	14.7721(7)	13.8014(6)	13.2777(6)	17.1283(10)
c [Å]	18.3583(7)	21.778(14)	16.7001(8)	18.8584(14)	16.1350(9)	21.6507(13)
a [°]	90	85.044(17)	88.0820(10)	90	84.604(2)	90
b [°]	90	79.313(18)	73.5710(10)	126.5450(10)	77.121(2)	91.366(2)
g [°]	90	89.59(2)	65.1440(10)	90	70.633(2)	90
V [Å ³]	4259.7(3)	2949(3)	2771.8(2)	5396.6(5)	2520.9(2)	5066.4(5)
D _c	1.407	1.265	1.483	1.511	1.529	1.538
Z	8	2	2	4	2	4
μ[mm ⁻¹]	2.017	0.257	0.589	0.652	0.590	0.589
Refl. measured	79348	169010	74501	15653	72138	103825
Refl. unique/R _{int}	4053/0.043	12063/0.050	11316/0.042	5491/0.028	9939/0.069	9276/0.170
Refl. with I > ns(I)	3399, n=3	11276, n=2	10685, n=2	5045, n=2	7672, n=3	5636, n=2.2
Nb parameters	253	728	712	336	649	556
R with I > ns(I)	0.0239	0.0625	0.0323	0.0325	0.0385	0.0808
R _w with I > ns(I)	0.0243	0.1433	0.089	0.0792	0.0403	0.0857
GooF	1.09	1.151	1.031	1.058	1.12	1.105
Dr _{max} /Dr _{min} [e.Å ⁻³]	0.44/-0.38	0.69/-0.57	1.82/-0.60	0.83/-0.56	0.74/-0.52	1.94/-1.73

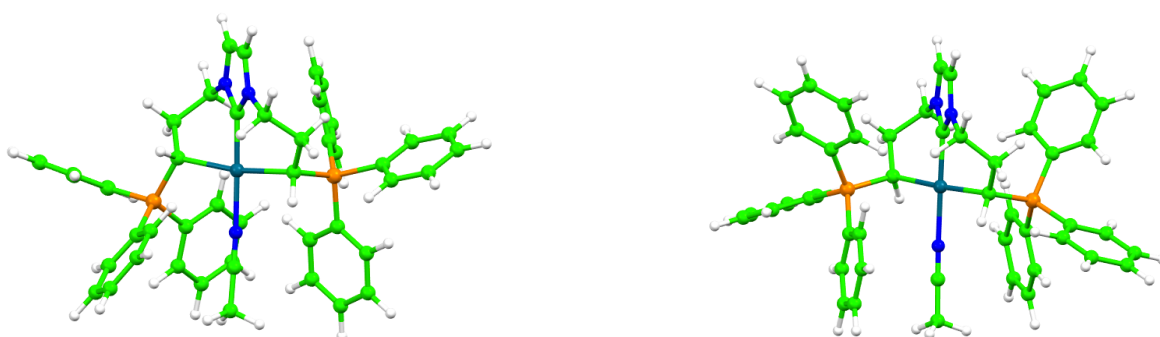
Computational details

Geometries were fully optimized at the PBE-D3/6-31G**/LANL2DZ* (Pd) level of calculation using Gaussian 09.¹ Vibrational analysis was performed at the same level as the geometry optimization in order to check the obtention of a minimum on the potential energy surface. Gibbs free energies were calculated at 298.15 K. Solvent effects of acetonitrile ($\epsilon = 35.688$) were included using the polarizable continuum model (PCM) implemented in Gaussian 09.

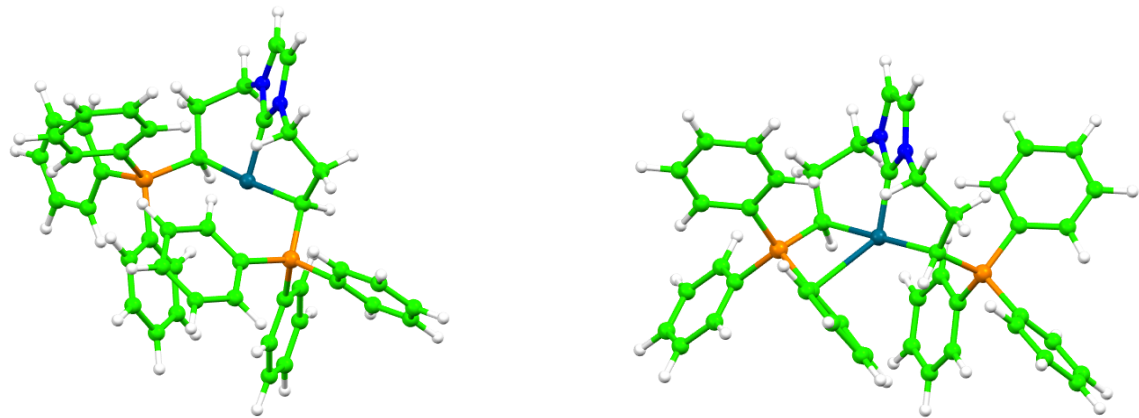
Optimized geometry of complex 7^+ at the PBE-D3/6-31G/LANL2DZ* (Pd) level of calculation: *cis*-isomer (left) and *trans*-isomer (right)**



Optimized geometry of complex 8^{2+} at the PBE-D3/6-31G/LANL2DZ* (Pd) level of calculation: *cis*-isomer (left) and *trans*-isomer (right)**



Optimized geometry of complex 8^{2+} at the PBE-D3/6-31G/LANL2DZ* (Pd) level of calculation: *cis*-isomer (left) and *trans*-isomer (right)**



¹ Gaussian 09, Revision D.01, M. J. Frisch, G. W. Trucks, H. B. Schlegel, G. E. Scuseria, M. A. Robb, J. R. Cheeseman, G. Scalmani, V. Barone, B. Mennucci, G. A. Petersson, H. Nakatsuji, M. Caricato, X. Li, H. P. Hratchian, A. F. Izmaylov, J. Bloino, G. Zheng, J. L. Sonnenberg, M. Hada, M. Ehara, K. Toyota, R. Fukuda, J. Hasegawa, M. Ishida, T. Nakajima, Y. Honda, O. Kitao, H. Nakai, T. Vreven, J. A. Montgomery, Jr., J. E. Peralta, F. Ogliaro, M. Bearpark, J. J. Heyd, E. Brothers, K. N. Kudin, V. N. Staroverov, R. Kobayashi, J. Normand, K. Raghavachari, A. Rendell, J. C. Burant, S. S. Iyengar, J. Tomasi, M. Cossi, N. Rega, J. M. Millam, M. Klene, J. E. Knox, J. B. Cross, V. Bakken, C. Adamo, J. Jaramillo, R. Gomperts, R. E. Stratmann, O. Yazyev, A. J. Austin, R. Cammi, C. Pomelli, J. W. Ochterski, R. L. Martin, K. Morokuma, V. G. Zakrzewski, G. A. Voth, P. Salvador, J. J. Dannenberg, S. Dapprich, A. D. Daniels, Ö. Farkas, J. B. Foresman, J. V. Ortiz, J. Cioslowski, and D. J. Fox, Gaussian, Inc., Wallingford CT, 2009.